ChinaSpec: a Network for Long-term *in situ* Measurements of Solar-induced Fluorescence and Reflectance in China

Y. Zhang[1,2*], Q. Zhang[1,2], L. Liu[3], S. Wang[4], W. Ju[1,2], J. Tang[5], X. Zhu[6], F. Wang[7], J. Zhang[8], G. Zhou[9], L. Zhou[9], X. Tang[10], Y. Huang[5], Z. Zhang[1,2], B. Qiu[1,2], X. Zhang[1,2], S. Wang[1,2]

[1]International Institute for Earth System Sciences, Nanjing University, Nanjing, Jiangsu 210023, China.

[2]Jiangsu Provincial Key Laboratory of Geographic Information Technology, Key Laboratory for Land Satellite Remote Sensing Applications of Ministry of Natural Resources, School of Geography and Ocean Science, Nanjing University, Nanjing, Jiangsu 210023, China.

[3]Key Laboratory of Remote Sensing Science, Institute of Remote Sensing and Digital Earth, Chinese Academy of Sciences, Beijing 100094, China

[4]Key Lab of Ecosystem Network Observation and Modelling, Institute of Geographic Sciences and Natural Resources Research, Chinese Academy of Sciences, Beijing 100101, China

[5]State Key Laboratory of Estuarine and Coastal Research, Institute of Eco-Chongming, East China Normal University, Shanghai 200241, China

[6]Key Laboratory of the Coastal and Wetland Ecosystems (Ministry of Education), College of the Environment and Ecology, Xiamen University, Xiamen, Fujian 361102, China

[7]Institute of Desertification Studies, Chinese Academy of Forestry, Beijing 100091, China

[8]Key Laboratory of Tree Breeding and Cultivation of State Forestry Administration, Research Institute of Forestry, Chinese Academy of Forestry, Beijing 100091, China

[9]State Key Laboratory of Severe Weather, Chinese Academy of Meteorological Science, Beijing 100081, China

[10]Chongqing Engineering Research Center for Remote Sensing Big Data Application, School of Geographical Sciences, Southwest University, Chongqing 400715, China

Corresponding author: Yongguang Zhang (yongguang_zhang@nju.edu.cn)

Key Points:

- A network of ground SIF measurements (ChinaSpec) is established.
- We presented an introduction on the current status and challenges of ChinaSpec
- ChinaSpec now consists of 15 tower sites including 5 cropland sites, 4 grassland sites, 4 forest sites and 2 wetland sites.

Abstract

Remotely sensed solar-induced fluorescence (SIF) has emerged as a novel and powerful approach for terrestrial vegetation monitoring. This *in situ* continuous optical remote sensing tool in conjunction with concurrent eddy covariance (EC) flux measurements provides a new opportunity to advance terrestrial ecosystem science. Here we introduce a network of ground-based continuous SIF observations at flux tower sites across the mainland China referred as ChinaSpec. Until now, it consists of 15 tower sites including 5 cropland sites, 4 grassland sites, 4 forest sites and 2 wetland sites. At each of these sites, an automated spectroscopy system was deployed to collect continuous *super-high* resolution spectra for high-frequency SIF retrievals in synergy with EC flux measurements. The goal of ChinaSpec is to provide ground SIF measurements and promote the collaborations between optical remote sensing and EC flux observation communities in China. We present here the details of instrument specifications, data collection and processing procedures, data sharing and utilization protocols, and future plans. Furthermore, we show the examples how ground SIF observations can be used to track vegetation photosynthesis from diurnal to seasonal scales, to assist in the validation of fluorescence models and satellite SIF products (e.g., from OCO-2, TanSat and TROPOMI) with the measurements from these sites since 2016. This network of SIF observations could improve our understanding of the controls on the biosphere-atmosphere carbon exchange and enable the improvement of carbon flux predictions. This SIF network will also help integrate ground SIF measurements with EC flux networks which will advance ecosystem and carbon cycle researches globally.

Keywords: ChinaSpec; Solar-induced chlorophyll fluorescence (SIF); Optical remote sensing; *In situ* continuous measurements; Eddy covariance flux; Terrestrial photosynthesis

1 Introduction

To understand the impacts of climate change, it is essential to monitor the dynamics of ecosystem carbon and water fluxes and their response to environmental changes in a warming world. The eddy covariance (EC) flux measurements have been widely used to quantify carbon, water vapor, and energy exchange between biosphere and atmosphere and improve our understanding of the variations in these fluxes (Baldocchi, 2008). The global EC network (FLUXNET) with more than 900 sites registered has been run for more than 20 years since 1990s (Baldocchi, 2019). However, the footprint of EC measurements is generally less than 1 km^2, and the sites are unevenly distributed around the world with biased spatial coverage towards flat topography and uniform ecosystem types. The insufficient spatial coverage of networks of EC flux sites makes it difficult to estimate gross primary productivity (GPP) of terrestrial ecosystem accurately at large scales. Therefore, from the global perspective, it is necessary to upscale tower-based observations of EC flux at the ecosystem level to regional and global levels.

Remote sensing (RS) offers a unique way to parameterize explicit plant information across multiple spatial scales, and thus improve simulations of carbon fluxes of terrestrial ecosystems at regional to global scales (Hilker et al., 2008). RS technique (e.g., MODIS sensor) have long been used for large-scale assessments of vegetation conditions, usually through the so-called vegetation indices (VIs) and other vegetation parameters derived from spectral measurements of surface reflectance (e.g. (Huete et al., 2002)). As a complement to reflectance-based VIs, solar-induced fluorescence (SIF) offers new possibilities to monitor vegetation function from space (Guanter et al., 2014). The recent technical advances have enabled the global SIF retrievals from satellites sensors. During the recent years, remote sensing of SIF has been proved to be a novel indicator of photosynthesis or GPP. There are growing number of space-borne missions with SIF retrievals that has opened up new possibilities to better monitor carbon flux and upscale EC flux data (Guanter et al., 2014; Frankenberg et al. 2011; Joiner et al., 2013; Köhler et al., 2015; Köhler et al., 2018; Sun et al., 2018; Du et al., 2018).

However, the fundamental mismatch in spatial scale remains a big challenge to upscale the EC flux data with satellite remote sensing data. Compared to the EC flux sampling, most satellite remote sensing data usually have coarse spatial and temporal resolution (e.g., MODIS). This sampling mismatch between remote sensing and flux measurements hinder the direct comparison between these two types of measurements. In this respect, *in situ* spectral measurements offer a unique opportunity to bridge the measurement gap between satellites and EC flux towers because they can be conducted at an appropriate scale that more closely matches the spatial and temporal scales of the EC fluxes. Numerous studies have shown the advantages of *in situ* measurements of spectroscopy to connect vegetation optical properties to flux measurements (Hilker et al., 2008; Porcar-Castell et al., 2015). The recent advances in sensor design and application have enabled the automated field optical sampling at the scale of flux tower footprints. With respect to the SIF measurements, a number of hyperspectral instruments has been deployed in the field since 2014 to support the rapid development of SIF retrievals from satellite missions (Yang et al., 2015; Yang et al., 2018a; Magney et al., 2019; Shan et al., 2019; Li et al., 2020). This is benefited from the advances in the commercially available spectrometers with high spectral resolution (e.g., QEpro from Ocean Optics, Inc., Dunedin, FL, USA), which enable the direct measurements of canopy SIF in the field. During the last few years, several novel ground-based SIF systems, including SFLUOR box (Cogliati et al., 2015), FluoSpec2

(Yang et al., 2018b), Photospec (Grossmann et al, 2018), FAME (Gu et al., 2019), FLOX (JB Hyperspectral Devices), SIFSpec (Du et al., 2019), Rotaprism (Josep A. Berry, personal communication), and SIFPrism (Zhang et al., 2019) have been developed and operated for autonomous continuous observations of canopy SIF in the field over years covering different vegetation types around the world. These SIF measurements are generally made together with EC flux observations providing opportunities for the integration between them and also for direct comparison and validation of satellite SIF data (Yang et al., 2015; Magney et al., 2019). Overall, ground-based spectral instruments could be used as a "bridge" between the EC flux and satellite remote sensing data.

Within this context, it is necessary to build a network with coordinated field spectral measurements concurrently with EC flux observations. Similar to the EC FLUXNET community (https://fluxnet.fluxdata.org/), several regional or global optical measurements have been established. For example, SpecNet (http://specnet.info) has been founded since 2003 for the integration of optical sampling with EC flux measurements across flux sites (Gamon et al., 2006; Gamon et al., 2010). Although this network has been stimulating an international collaboration between remote sensing and flux communities, the field sites are mainly located in North America (NA). Recently, the European remote sensing community has also started to establish its own optical network, EUROSPEC, to conduct long-term *in situ* optical measurements at the representative EC towers in the European Union (EU) (Porcar-Castell et al., 2015). The EUROSPEC plays a fundamental role in supporting the European satellite mission like the Fluorescence Explorer (FLEX). Overall, these networks are mainly covering the geographical areas of EU and NA. Not until very recently, the Chinese remote sensing and EC flux communities have started to conduct *in situ* spectral measurements.

In China, a network of collaborating sites and investigators has been founded to conduct *in situ* continuous optical measurements along with EC flux for ecosystem research since 2017. The network is referred as ChinaSpec (http://chinaspec.nju.edu.cn). The goal of ChinaSpec was to promote the integration of optical measurements, especially the novel SIF measurements, with EC flux measurements for better understanding the controls of climate and environmental factors on the biosphere-atmosphere fluxes of carbon and water vapor in China. A primary goal of ChinaSpec is to collect the long-term continuous SIF measurements in the field over different vegetation types across the country, and to fill the gap between EC flux and satellite SIF observations.

The overall aim of this paper is to present an introduction on the current status and challenges in the ChinaSpec network. A primary ChinaSpec focus is on the ground SIF measurements at the flux sites within ChinaFLUX network (http://www.chinaflux.org/) (Yu et al., 2006; Yu et al., 2010), where the EC measurements have existed for more than 10 years. Specifically, we emphasize on the current status of ChinaSpec and provide the usefulness of such network datasets for future research directions.

2 Instrumental Set-up

2.1 Instrument configurations

1) Instrument description

In the network of ChinaSpec, we mainly used hyperspectral spectrometers to conduct *in situ* continuous hyperspectral measurements, in particular SIF measurements above the canopy. The spectrometer used for SIF observation is QEPro or QE65Pro (OceanOptics, Inc., Dunedin, FL, USA). QEPro is an improved type of QE65Pro with high saturation threshold with digital number (DN) up to 200,000 (65535 for QE65Pro). Currently, several SIF systems are used in the network. Fluospec2 (Li et al., 2020; Yang et al., 2018b) and SIFSpec (Du et al., 2019) are the widely used systems in the ChinaSpec network (Figure 1). Another spectrometer HR2000+ (OceanOptics, Inc., Dunedin, FL, USA) covering spectral range from 300 nm-1000 nm is often used to measure hyperspectral canopy reflectance, but only available from a few sites in ChinaSpec (Table 1). A temperature-controlled waterproof box is used for housing the two spectrometers and keeping the environment temperature around 25 °C to reduce instrument-noise. As spectrometer having only one input optical path, a "Y-shaped" splitter fiber-optic separating one optical path into two paths, and a fiber-optic shutter TTL (OceanOptics, Inc., Dunedin, FL, USA) switching between two input fibers are used to enable the spectrometers to nearly-simultaneously measure both solar irradiance and canopy radiance (Figure 1). One of the two input fibers is fixed upward for measuring the downwelling solar radiation equipped with cosine corrector CC-3 (OceanOptics, Inc., Dunedin, FL, USA), and another one is a bare fiber to collect the upwelling canopy radiation (Figure 1).

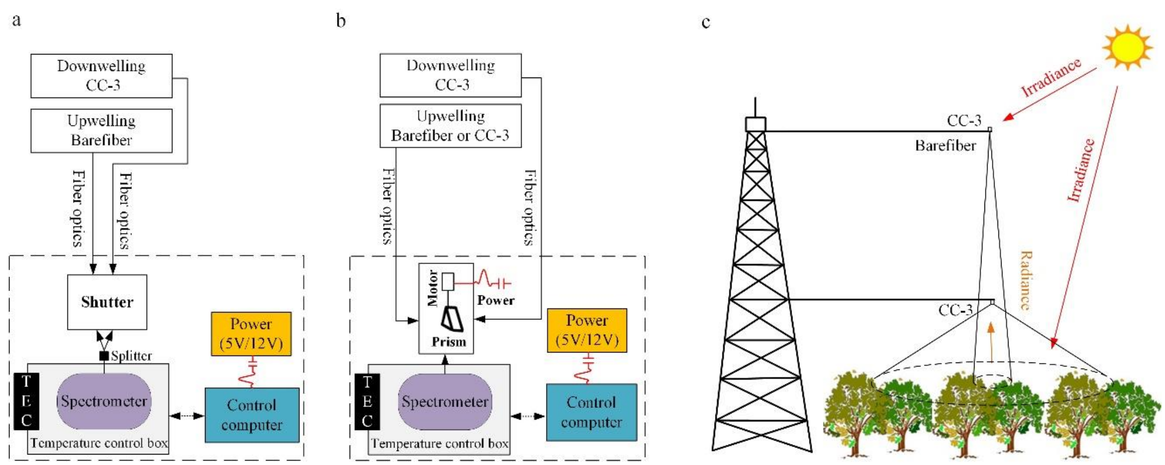

Figure 1. Schematic layout of the hyperspectral instrument used in ChinaSpec. (a) Fluospec2 or SIFspec system. (b) SIFprism system. (c) A drawing of field configurations for *in situ* spectral measurements with upwelling bare fiber or cosine corrector CC-3.

A newly developed system called SIFprism (Zhang et al., 2019) is also deployed in some sites of the ChinaSpec network (Figure 1b). A rotary prism, which is rotated by an electric motor, built inside a sealed and adiactinic box is used to collect both solar and canopy radiation sequentially as a replacement of TTL. Output light of prism goes into the spectrometer via a single-core fiber-optic (Figure 1b). SIFprism has been tested for a growing season at a paddy-rice site in 2019 and will be promoted in ChinaSpec network.

Both hemispherical-conical (with conical upwelling sensor, i.e. bare fiber optic) and bi-hemispherical configurations (with hemispherical upwelling sensor, i.e. bare fiber optic with cosine corrector CC-3) can be adapted to Fluospec2 and SIFprism. The efficiency of SIFprism is much higher than that of Fluespec2 and SIFSpec. Therefore, SIFprism is easy to be adopted with bi-hemispherical configuration (Figure 1c) to view a larger field of the canopy even with lower height than conical upwelling sensor (Zhang et al., 2019). This is more relevant to the footprint of EC flux measurements.

2) Data collection and processing

All systems can automatically operate and collect spectral data under various field conditions. Solar irradiance (*E*) and canopy radiance/irradiance (*L*) are sequentially acquired, or a sandwich-method (*E*-*L*-*E*), which is helpful for evaluating if changes in illumination suitable for SIF observation during this short period, is used to measure spectral data (Li et al, 2020; Zhang et al., 2019). Dark current (DC) is simultaneously recorded after each spectral measurement for DC correction. Integration time (IT) of spectral measurement is automatically optimized to get as high and unsaturated values as possible to improve the signal-to-noise (SNR) ratio:

$$IT = IT_{ini} \times targetDN / maxDN \tag{1}$$

where IT_{ini} is user-defined initial *IT*; *targetDN* is about 60%-80% of the saturation DN value of the spectrometer; *maxDN* is the maximum value of a spectrum acquired with IT_{ini} at the beginning of each measurement.

Spectral data is recorded as DN values, which need to be radiometrically calibrated. Pre-mounted laboratory calibration using a tungsten halogen light source (HL-CAL-2000, Ocean Optics, USA) is conducted to calibrate hemispherical sensor (CC-3) and an integrated sphere to calibrate conical sensor (bare fiber) (Zhang et al., 2019). To monitor the status of optical paths under changeable field conditions, regular radiometric calibration is generally performed in the field using light source to calibrate CC-3 and a well-calibrated spectrometer with a standard reference panel (Spectralon, Labsphere, NH, USA) to calibrate bare fiber under a clear sky day around noon. The conversion of DN to radiance or irradiance can be finally expressed as (take radiance as an example):

$$Radiance(\lambda) = \frac{L(\lambda) \times \left(DN_{obs}(\lambda) - DC_{obs}(\lambda)\right) \times IT_{cal}}{\left(DN_{obs}(\lambda) - DC_{obs}(\lambda)\right) \times IT_{obs}} \tag{2}$$

where λ represents the wavelength, *L* is the calibrated radiance, the subscript *obs* means the field observation data recorded by the spectrometer and *cal* represents the calibration data. Both *DN* and *DC* are normalized by the IT used in each measurement to one second.

Data quality control is operated before SIF retrieval following the protocol presented by (Cogliati et al., 2015) to exclude abnormal data caused by changing weather conditions and other unpredictable reasons. The approaches used for SIF retrieval include three-band Fraunhofer Line Depth (3FLD, (Maier et al., 2003)) and Spectral Fitting Methods (SFM, (Meroni & Colombo, 2006)). The 3FLD algorithm stems from the FLD principle, which requires spectral measurements at two bands, one inside and one outside a Fraunhofer line (Theisen, 2002). The FLD method assumes that the reflectance (hereafter, *r*) and SIF maintain constant at the two bands. However, in fact, the two variables are far from being constant, especially for *r* at 687 nm and SIF at 760 nm. Therefore, the FLD assumption has been questioned by several authors (Meroni & Colombo, 2006; Alonso et al., 2008; Gómez-Chova et al., 2006; Meroni et al., 2009; Moya et al., 2006). The 3FLD method is based on an advanced assumption compared with FLD, namely the r and SIF vary linearly in the spectral domain considered, which overcomes the limitations given by FLD assumptions (Meroni et al., 2009). The 3FLD-based SIF at 760 nm can been derived as:

$$SIF_{760} = \frac{(E_{left} \times w_{left} + E_{right} \times w_{right}) \times L_{760} - (L_{left} \times w_{left} + L_{right} \times E_{right}) \times E_{760}}{(E_{left} \times w_{left} + E_{right} \times w_{right}) - E_{760}} \quad (3)$$

Where w_{left} and w_{right} denote the weight of the band, which is proportion to the length between the right/left band and the inner band. The subscripts “left” and “right” represent the band at the left and the right of the absorption domain.

Differently, SFM employs two mathematical functions to describe r and SIF, which relaxes the assumptions of some FLD-based methods (Meroni et al., 2009). Here, we use two linear functions to determine r and SIF in a restricted spectral domain around the O_2 absorption bands. Therefore, L(λ) can be expressed as:

$$L(\lambda) = \frac{r_{mod}(\lambda)E(\lambda)}{\pi} + SIF_{mod}(\lambda) + \varepsilon(\lambda) \quad (4)$$

where $r_{mod}(\lambda)$ and $SIF_{mod}(\lambda)$ are linear functions describing r and SIF, respectively. $\varepsilon(\lambda)$ represents the error between the simulated and observed L(λ). With a large number of very high spectral observations pledged by very high spectral resolution spectrometers and continuous measurements, the Eq. (4) can been overdetermined. Least square method is applied to solve the parameters (i.e. the respective gain and offset of $r_{mod}(\lambda)$ and $SIF_{mod}(\lambda)$) in the two functions. Then, SIF at 760 nm can been determined as $SIF_{mod}(760)$.

2.2 Field set-up

The SIF observations systems are generally mounted on the flux tower with EC systems (Figure 2). At some sites with tall towers, the observation systems can be easily mounted on the tower as high as possible to gain a large field of view (FOV). At the sites with short canopy (e.g., crops), a simple self-made or commercial bracket is needed to hold the fiber optics steady. The ends of fiber optics, where the solar and canopy radiation penetrating into the system, are better to be way off the tower or bracket to avoid their optical signal interfering the signal of interest. Therefore, the fiber optics are extended along with horizontal-setup pipe (or equivalent devices, such as sectional bar) about 2-4 m away from the edge of the platform depending on the FOV of the upwelling sensor.

At present, SIF observation systems used at most sites are Fluospec2 or SIFspec of hemispherical-conical configuration. The downwelling fiber optics with CC-3 are vertically mounted on a horizontal metal plate or an anti-dust (using fan) installation device (also helpful for avoiding insects and birds) fixed on the pipe. The upwelling bare fibers are mounted on a horizontal metal plate nadir or off-nadir fixed at the end of the pipe. The view zenith angle of the upwelling sensor is recommended less than 10° to constrain the effects of sun-viewer geometry variability. To avoid the influence of the shadow of the tower or the bracket, the horizontal pipe should point to the south. Starting from 2019, SIFprism (Zhang et al., 2019) was also installed at two sites (JR and ZLQ in Table 1) with bi-hemispherical configurations.

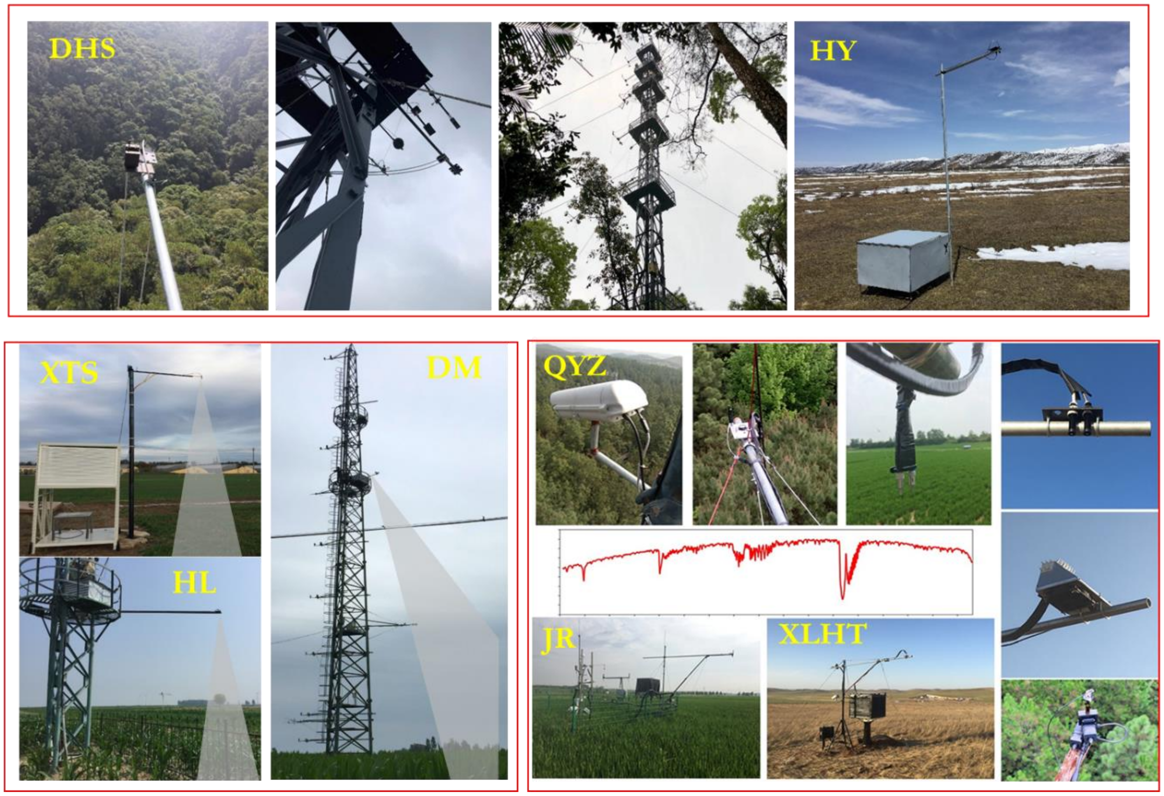

Figure 2. Examples of field set-up at several sites in ChinaSpec. The abbreviation of each site is referred in the next Section (Table 1).

3 Current status of ChinaSpec

3.1 Field SIF sites in China

Up to now, 15 sites have registered with ChinaSpec network, including 5 cropland, 4 grassland, 4 forest and 2 wetland sites across from subtropical to cold temperate zones and also covered from humid to semiarid regions (Figure 3 and Table 1). The altitudes of the sites vary from sea level up to more than 3000 m. Locations of the 15 sites are shown in Figure 3, and detailed information of each site can be found in Table 1. The spectrometers used for SIF observation in these sites might be different (QEpro or QE65pro), but are all suitable for collecting SIF signals. The spectral range of these devices covers the range for far-red SIF (760 nm) and some of them cover both red SIF (687 nm) and far-red SIF.

The five cropland sites are distributed on the Zhangye oasis in northwest of China (DM), Central plain (SQ), Yangtze plain (JR) and North China plain (HL and XTS) that monitor maize, rice and winter wheat. HL and DM have only one growing season in a year which plants maize in the summer. DM is located in temperate semiarid region, different with HL belonging to temperate semi-arid region. XTS and SQ belong to the continental monsoon climate having sufficient hydrothermal supply suitable for winter wheat and maize rotation cultivation. **SQ** is located at Henan Province (34.5199 N, 115.5916 E, and about 55 m in elevation) and is a summer maize (*Zea mays*)-winter wheat (*Triticum asetivum*) cropping system, with average annual total precipitation is 704 mm, and average annual air temperature is approximately 14 ℃. **JR** (31˚48'24.59"N, 119˚13'2.15"E, elevation 15 m) is the unique site for rice observation, growing rice and winter wheat. The climate at JR is northern subtropical semi-humid monsoon climate, where the mean annual temperature of 15.2 ℃ and mean annual precipitation of 1058.8 mm. SIFprism, the newly developed SIF system, has been also deployed at JR site since June, 2019.

Among the four forest sites, DHS is an evergreen broadleaf forest and QYZ is an evergreen needle forest. Both sites locate in the sub-tropical area with abundant rainfall and solar radiations. **DHS** (240 m asl) is located in the kernel area of Dinghushan National Reserve, Guangdong Province, South China. The region has a subtropical monsoon humid climate, with an average annual temperature and total precipitation of 20.9 ℃ and 1956 mm, respectively. The dominant tree species include *Schima superba*, *Castanopsis chinensis*, *Pinus massoniana* etc., with mean canopy height of around 18 m. The soil mainly consists of lateritic red-earth (Wang et al., 2006). **The QYZ site** (100 m asl) is located in Taihe County, Jiangxi province, which is the typical hilly red soil region in the mid-subtropical monsoon landscape zone of South China. The mean annual air temperature is 18.6 ℃ and mean annual precipitation is 1488 mm, respectively. The vegetation cover is planted coniferous forest since 1983 with dominate species of *Pinus elliottii*, *Pinus massoniana*, *Cunninghamia lanceolata* and *Schima superba* etc. **The BB site** consists of managed pure *Osmanthus fragrans* stand, which is green nearly throughout the year (Yang et al., 2009). Climate of this site is subtropical monsoon humid. Multi-year mean temperature and precipitation are 16.5 ℃ and 1250 mm, respectively. Over 70% of annual rainfall is concentrated during May to August. **The XLD site** locates at Jiyuan county, Henan province (410 m asl), with a warm-temperate continental monsoon climate (mean annual air temperature of 13.4 ℃). Annual rainfall is 642 mm and about 70% of precipitation falls in July-September. The forest stand is dominated by cork oak (*Quercus variabilis blume*) (80%), black locust (*Robinia pseudoacacia L.*) (12%) and arborvitae (*Platycladus orientalis*) (8%). The area of the 32-yr mixed plantation is approximately 7210 ha, with the stand density of 1905 trees ha^{-1}. The canopy has an average height of approximately 10.2 m. Maximum leaf area index (LAI) is close to 7.0 in the growing season (April–September) of the mixed plantation (Tong et al., 2019).

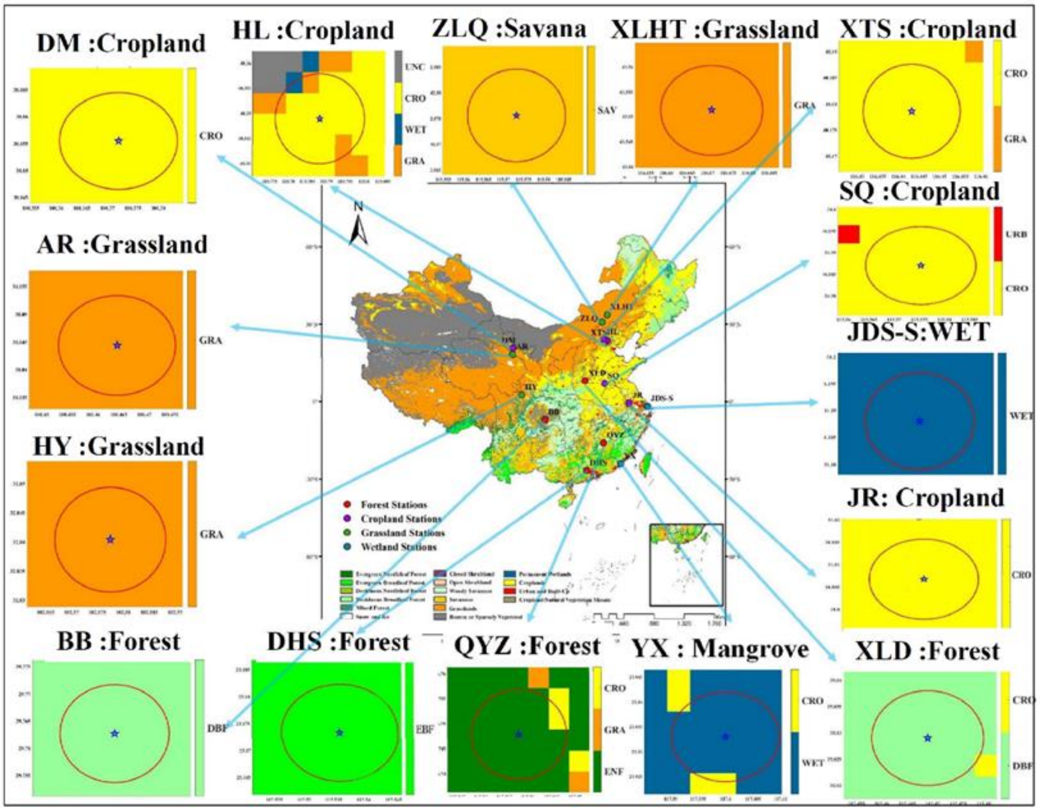

Figure 3. Summary of current field SIF sites in the network of ChinaSpec. The name of each site is referring in Table 1. The subplots are the surrounding vegetation type at each of the 15 sites (blue star). The base map is the land cover map based on the MODIS Land Cover Type product (MCD12C1) with the IGBP land cover classification scheme at a spatial resolution of 500 m.

The four grassland sites include two alpine meadow (HY and AR), one semi-arid grassland, and one sparse forest grassland. **HY** is located in an alpine meadow of the eastern Qinghai-Tibetan Plateau (3500 m asl) in Hongyuan County, Sichuan. The region is characterized by a temperate continental monsoon climate. The average annual temperature is 1.1℃ and annual precipitation is 753 mm, with around 80% occurring during May to September. Plant species in the alpine meadow are dominated by *Deschampsia caespitosa* (Linn.) *Beauv.*, *Koeleria cristata* (Linn.) *Pers.*, *Gentiana sino-ornata Balf. f.*, *Potentilla anserina L.*, and *Anemone rivularis Buch.-Ham*. The soil is dominated by subalpine meadow soils, and peat moor soils (Quan et al., 2019). The **XLHT** site (116°42′ E, 43°38′ N, 1250 m asl) is located at the Xilin River Basin, Inner Mongolia, called the Inner Mongolia Grassland Ecosystem Research Station. It is semiarid continental climate with mean annual air temperature (1980-2012) of 0.3 ℃ and annual precipitation of 346 mm with more than 80% occurring during the growing season (May-October) (Zhang et al., 2016). This site has been fenced since 1999 and no grazing or other disturbance thereafter. Vegetation in this site is a typical steppe and dominated by perennial grasses (*Leymus chinensis* and *Stipa grandis*). **The ZLQ site** is Elm Sparse Forest Grassland Ecosystem (1300 m asl), which also located in the north-east of Otingdag Sandland, Inner Mongolia, northeastern China. The annual average temperature of 1.8 ℃. The average annual rainfall of 313.8 mm and summer precipitation takes over 68.3%. The typical vegetation is natural sparse elm (*Ulmus pumila*) forest, shrubs and grass (Wang et al., 2019). **The AR site** is located in the Heihe River Basin. The altitude of AR is higher than 3000 m, and the vegetation cover is alpine meadow. There is an EC flux tower in AR, therefore the observation is mounted at a tall height (25 m). Its climate belongs to a typical temperate continental climate. The average annual temperature is 0.7 ℃, and the annual total precipitation is 400 mm. The dominant vegetation is alpine meadow, and the soil type is a chestnut soil, loam.

In addition to forest, cropland and grassland sites, there are two wetland sites (JDS-S and YX) in ChinaSpec, which are very unique ecosystems for SIF measurements. **JDS-S** is a coastal salt marshes site located in the Jiuduansha Shoal of Yangtze estuary to the East China Sea. Jiuduansha emerged in 1950's and have been developed as a stable island over a half century. JDS-S is dominated by *Spartina alterniflora* with 2 m height during the growing season. This site is featured by semidiurnal tides, and regularly flooded and drained by saltwater brought in by the tides. **The YX site** is located in the area of Zhangjiang estuary to the South China Sea. It is a subtropical intertidal wetland vegetated with mangrove forests mainly comprised of *Kandelia obovate*, *Avicennia marina*, and *Aegiceras maizeiculatum*. The site has a monsoon climate with annual rainfall of 1714 mm mostly occurring from April to September, mean air temperature of 21.2 ℃ and relative humidity of 79%. The wetland experiences an irregular semidiurnal tide with annually mean tide range of 2.3 m and varying tidal water salinity up to 15 PSU. High tides can reach up to ~1 m above sediment surface at the flux tower, and the sediment surface is also exposed for days during the annual minima. The biggest challenge of observation for these two sites is the protection of the observation systems from humid and salty air to avoid corrosion of metal components.

Table 1. Information of the field sites in ChinaSpec

ID	Site Name	Site ID	Location	Coordinate	Height*	PFT	Instrument	Spectral range	Time Period
1	XiaoTangShan	XTS	Beijing	40.1786 N 116.4432 E	4 m/2.6 m	Cropland (winter wheat and maize rotation)	SIFSpec with QE65pro	650- 800 nm	06/2017-
2	HuaiLai	HL	Hebei Province	40.3489 N 115.7882 E	2.5 m	Cropland (maize)	SIFSpec with QE65pro	650- 800 nm	0-/2017-
3	DaMan	DM	Gansu Province	38.8555 N 100.3722 E	23 m	Cropland (maize)	SIFSpec with QE65pro	650- 800 nm	05/2017-
4	ShangQiu	SHQ	Henan Province	34.5870 N 115.5753 E	12 m/ 10 m	Cropland (winter wheat and maize rotation)	FluoSpec2 with QEpro and HR 2000+	730-780 nm	07/2017-
5	JuRong	JR	Jiangsu Province	31.8068 N 119.2173 E	8 m	Cropland (winter wheat and rice rotation)	FluoSpec2 with QEpro and HR 2000+	730-780 nm	07/2016-
6	QianYan Zhou	QYZ	Jiangxi Province	26.7478 N 115.0581 E	15 m	Evergreen coniferous forest	FLOX with QEpro	650- 800 nm	Only 2017
7	XiLinhot	XLHT	Inner Mongolia	43.5513 N 116.6710 E	2.5 m	Grassland	FluoSpec2 with QEpro and HR 2000+	730-780 nm	06/2017-
8	DingHuShan	DHS	Guangdong Province	23.1733 N 112.5361 E	18 m	Evergreen broadleaf forest	SIFSpec with QEpro	650- 800 nm	08/2017-
9	HongYuan	HY	Sichuan Province	32.8404 N 102.5775 E	3 m	Alpine meadow	SIFSpec with QEpro	650- 800 nm	04-07/2018
10	A’Rou	AR	Qinghai Province	38.0444 N 100.4647 E	25 m	Alpine meadow	SIFSpec with QE65pro	650- 800 nm	04/2019-
11	YunXiao	YX	Fujian Province	23.9240 N 117.4147 E	7 m	Mangrove	FluoSpec2 with QEpro and HR 2000+	730-780 nm	01/2018-
12	BeiBei	BB	Chongqing	29.7627N 106.3191E,	10 m	Managed Forest (Osmanthus)	SIFSpec with QE65pro	650- 800 nm	9/2018-
13	ZhengLanQi	ZLQ	Inner Mongolia	42.9656N 115.9589E	2 m	Sparse forest grassland	SIFSpec with QEpro	730-780nm	6/2019-
14	XiaoLangDi	XLD	Henan Province	35.029 N 112.469 E	20 m	Deciduous broadleaf forest(oriental oak)	SIFSpec with QE65pro	650- 800 nm	6/2019-
15	Jiuduansha-S	JDS-S	Shanghai	31.1881N 121.9489E	2 m	Coastal wetland *(Spartina)*	SIFSpec with QE65pro	650- 800 nm	3/2019-
16	GuCheng	GC	Hebei Province	39.1333 N, 115.6667 E	5 m	Cropland (winter wheat and maize rotation)	SIFprism with QEpro	650- 800 nm	3/2020#

*** Height above the canopy; # The SIF system will be installed in the spring of 2020 at a cropland site.**

3.2 Data policy

ChinaSpec collaborates with the network of ChinaFLUX and other communities, and shares ground spectral and SIF data acquired from the sites of the network. The website (Figure 4, http://chinaspec.nju.edu.cn) is the platform for releasing the related information and sharing datasets of the sites registered in the ChinaSpec network since 2016 when the first dataset was collected. The dataset consists of metadata of each site, reflectance covering spectral range from 400 nm to 1000 nm (if available), retrieved SIF with two methods (3FLD and SFM) after data quality control. A few sites could also share EC measured data (includes CO2, H2O and energy fluxes, as well as meteorological measurements such as radiation, air temperature, relative humidity, precipitation, wind speed and direction), but EC flux data at most sites are generally shared through ChinaFLUX network (Yu et al., 2006; Yu et al., 2010). The temporal scale of the dataset is half hourly, which is processed from high frequency raw data (~1 minute for spectral data).

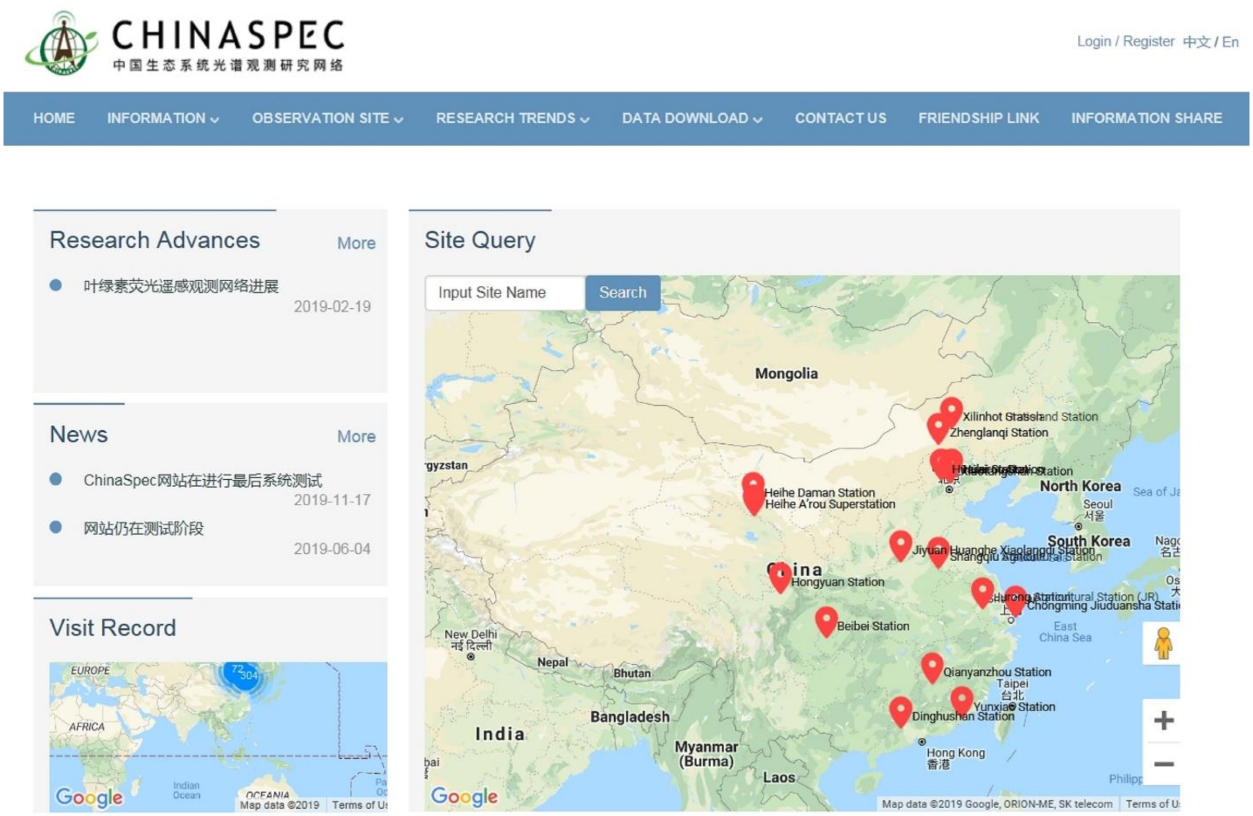

Figure 4. Website of ChinaSpec (http://chinaspec.nju.edu.cn). Introduction, data sharing and other information are provided through this website.

The intent of sharing this dataset is to provide continuous *in situ* SIF and reflectance measurements across multiple ecosystems in China to the broad community of scientists who need ground observations to improve the understanding the controls on the biosphere-atmosphere fluxes of carbon and water vapor based on remote sensing approaches, especially on the SIF observations. As all sites are operated by their own funding of PIs, the ChinaSpec dataset only provide the dataset that PIs who give us the permission to share their datasets over these SIF measurement sites in China. We hope that this platform and dataset shared by ChinaSpec network will promote the developments of the methods and data quality of spectral measurements, and enable a new perspective of integrating spectral and EC measurements with the aim to increase the quality of the research and the collaboration on ecology and optical remote sensing communities.

The data usage polices for ChinaSpec is similar to that for FLUXNET dataset (especially the FLUXNET2015 Dataset). The use of spectral data in ChinaSpec will follow "the fair use policy" (https://fluxnet.fluxdata.org/). In other words, the ChinaSpec datasets are open and freely available for scientific and educational purposes by any registered user after acceptance of a proposal (at least 200 words to describe the intention of using this dataset) submitted to the steering committee. That is, data users submit a small proposal on the intended use of the data before they download the data; this intended-use statement will be emailed to the data producer(s) of the sites. This policy means that "(1) data producers are informed of who uses the data and for what purpose and (2) that proper acknowledgment and citations are given to all data used in a peer reviewed publication, via the following protocols: providing a co-authorship to the site PIS or at least a citation of a publication for each site". It is requested that every publication specifies each site used with the data-years used and brief acknowledgment for funding (if provided by ChinaSpec PI) in the text. We recommended the users to contact the site PIs before publishing to avoid potential misuse or misinterpretation of the data. In particular, if a work is based on the SIF data from only a few sites, it is strongly recommended to contact the site PI about coauthorship or proper acknowledgment for their contribution.

The distribution of the data for each site will be shared after the first publication or two years later after data collections. At this stage, the data we share for each site is ground far-red SIF (760 nm) retrievals with 3FLD and SFM algorithms and vegetation indices (e.g., NDVI, EVI, and PRI depending on sites) at half-hourly time scales. Since the year of 2019, we have distributed the spectral dataset including reflectance and SIF for 1-2 years from 6 sites. The rest of the spectral dataset will be regularly updated with data from new site years.

4 The usefulness of networking SIF observations

The ground spectral and SIF measurements collected in ChinaSpec are not only essential for the integration of optical remote sensing and EC flux data across space and time, but also for investigating the dynamics of canopy SIF and its link to GPP across multiple spatial and temporal scales. These continuous ground measurements of SIF are also benefiting the validation of fluorescence models and satellite SIF retrievals.

4.1 Diurnal and seasonal dynamics of canopy SIF across different ecosystems

There are growing interests on how SIF changes with radiations and GPP across different ecosystems. Among the fifteen sites in the ChinaSpec network, eight sites were selected as an example to investigate the relationships of SIF with photosynthetically active radiation (PAR) and GPP at diurnal scale. Diurnal patterns of far-red SIF, PAR and GPP under clear sky conditions from four cropland site (one is rice and the other three are maize), two wetland (one is coastal marsh and the other is mangrove), one grassland and one forest (EBF) sites are shown in Figure 5. At all of these four cropland sites (JR, SQ, DM and HL), SIF closely varied with both PAR and GPP, which indicates that SIF and GPP were both driven by PAR under the clear sky conditions. At the grassland site (XLHT), the variations of SIF were slightly divergent with GPP while PAR was stable, probably due to the fast moving clouds that may cause fluctuation of radiations at this site. Similar with cropland site, SIF was closely related with both PAR and GPP at the coastal marsh site. However, at another wetland site (YX, mangrove), SIF varied with PAR under low light but fluctuated under high light (around noon), while the diurnal pattern of GPP was divergent with SIF and PAR, probably owing to the relative heterogeneous canopies. For the broadleaf forest, SIF mostly varied with GPP. However, SIF and GPP obviously decreased in the afternoon even PAR level was higher than that in the morning, partly owing to the physiological changes and diurnal variations of sun-viewer geometry. These results demonstrate the potential of ground SIF measurements for understanding diurnal canopy SIF variations across sites, and also highlight the importance of networking on SIF measurements.

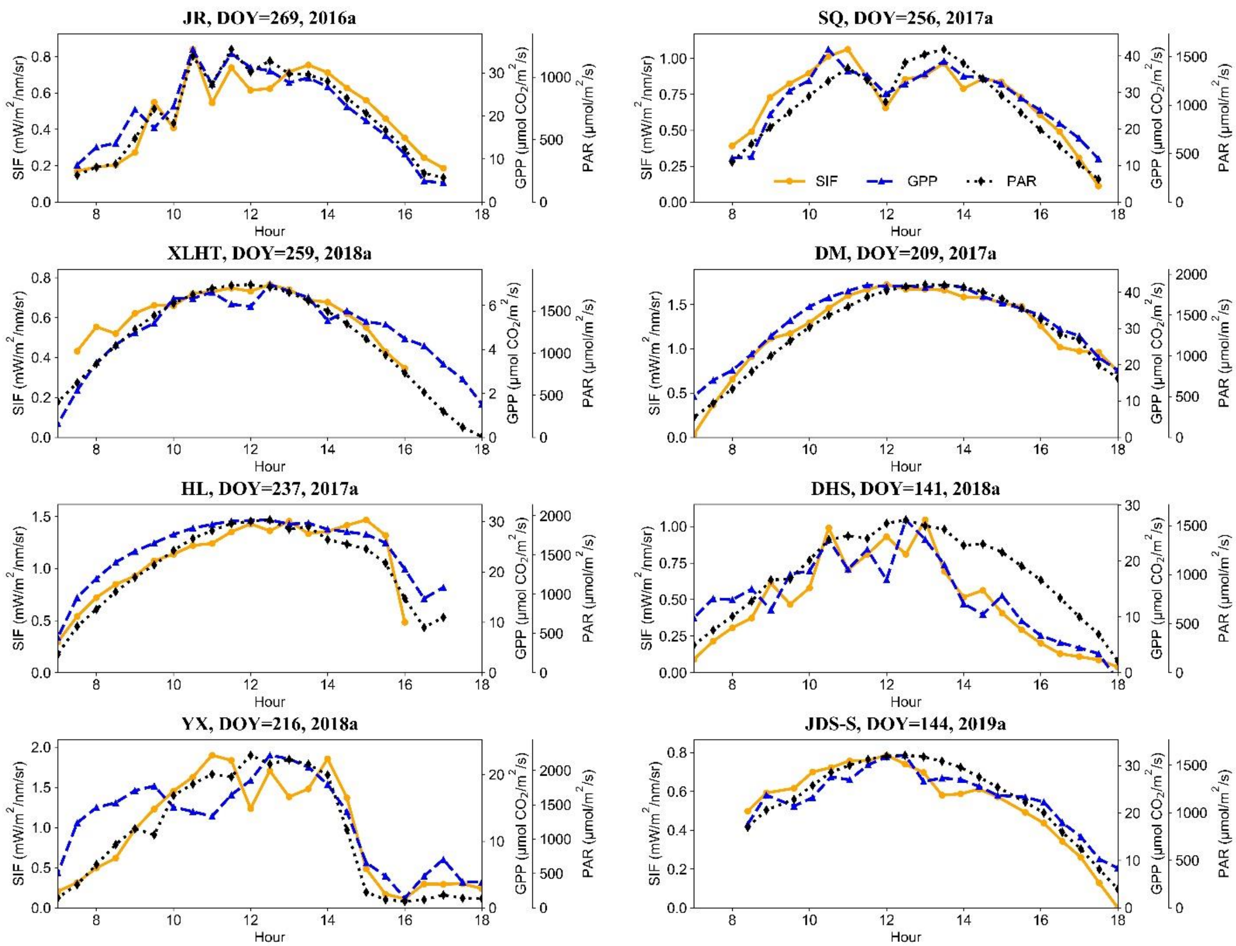

Figure 5. An example on the diurnal variations of SIF, PAR, NDVI and GPP at eight SIF sites. For each site, we chose one clear-sky condition for illustration. The name of each site is referring in Table 1.

At seasonal scale, SIF has been proved to be the best indicator of GPP while reflectance-based NDVI could only represent greenness of the canopy. As an example, Figure 6 displays the seasonal variations of SIF, NDVI, GPP and PAR at four sites including three croplands and one grassland. During the growing season, the seasonal dynamics of SIF, GPP and PAR of rice (JR) were generally consistent, while NDVI was generally stable. For maize at the SQ and DM sites, SIF varied synchronously with GPP, which could capture the increase of GPP at the start stage of the growing season (DM) and decrease at the end of the growing season (SQ) when PAR was staying at a high level. NDVI increased with GPP and SIF at the beginning of the growing season (DM), but still kept in high values (SQ) after SIF and GPP decreased after day 240, and started to decline until SIF and GPP approaching zero possibly contributed to plant LAI stayed stable until the very end of the growing season. Since canopy structure of the grassland is rather simple, NDVI of grassland showed a generally clear seasonal pattern similar to SIF and GPP. However, the variation of SIF was greater than that for GPP because of the fluctuation of PAR.

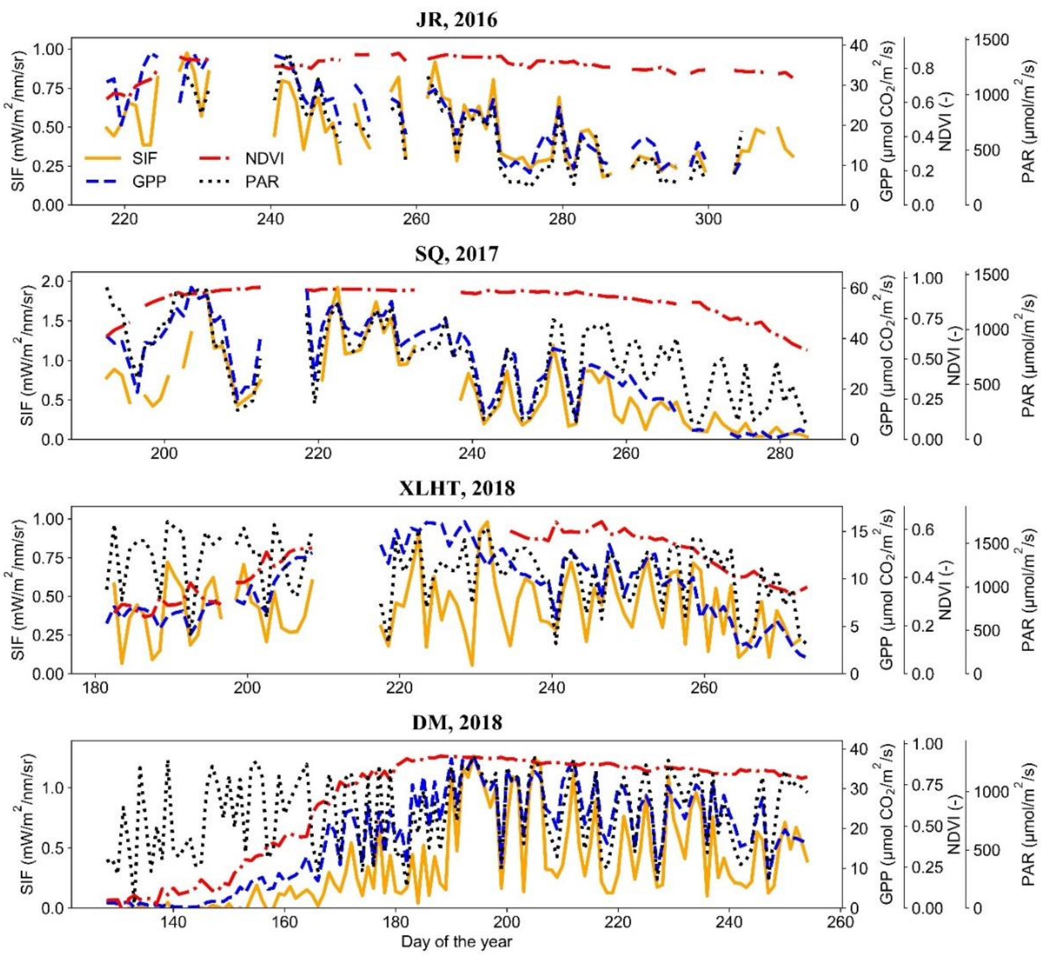

Figure 6. Seasonal variations of SIF, PAR, GPP and NDVI at 4 SIF sites for one-year measurements. The name of each site is referring in Table 1.

4.2 Synthesis of diurnal SIF-GPP relationship across multiple sites

Ground-based SIF observations have been conducted in different ecosystems globally, and different relationships between SIF and GPP have been reported (Yang et al., 2015; Damm et al., 2015). Even for a single ecosystem, the correlation between SIF and GPP may change at different growing stages (Yang et al., 2018a; Li et al., 2020). Figure 7 shows significant diverse slopes of relationships between SIF and GPP (left) but comparable relationships between SIF and PAR (right) at the diurnal scale across seven sites including four croplands, one forest, one grassland and one mangrove. The SIF-GPP correlations for croplands (JR, DM, SQ and HL) are stronger than other ecosystems. The SIF-GPP correlation is weaker than SIF-PAR at XLHT due to variations of illumination conditions. On the opposite, SIF-GPP relationship is stronger than that of SIF-PAR at DHS site, which suggest that SIF is able to capture the seasonal variations of GPP in this sub-tropical evergreen broadleaf forest and its relationship with PAR may different in wet and dry seasons at this area. The inconsistent relationships between SIF and GPP across different ecosystems may be attributed to different canopy structures. The regression slopes of SIF with PAR from different sites have less variations, which demonstrate that SIF-GPP relationships are affected by canopy structure in different ways. Additionally, SIF is also affected by escape probability due to multiple scattering in far-red region. This indicates the necessity to expand SIF observations covering a variety of ecosystems to investigate and improve the ability of SIF for monitoring photosynthesis. With the growing SIF observations in ChinaSpec over multiple ecosystems, further deep synthesis work could be done for better understanding the link between SIF and GPP at different temporal and spatial scales.

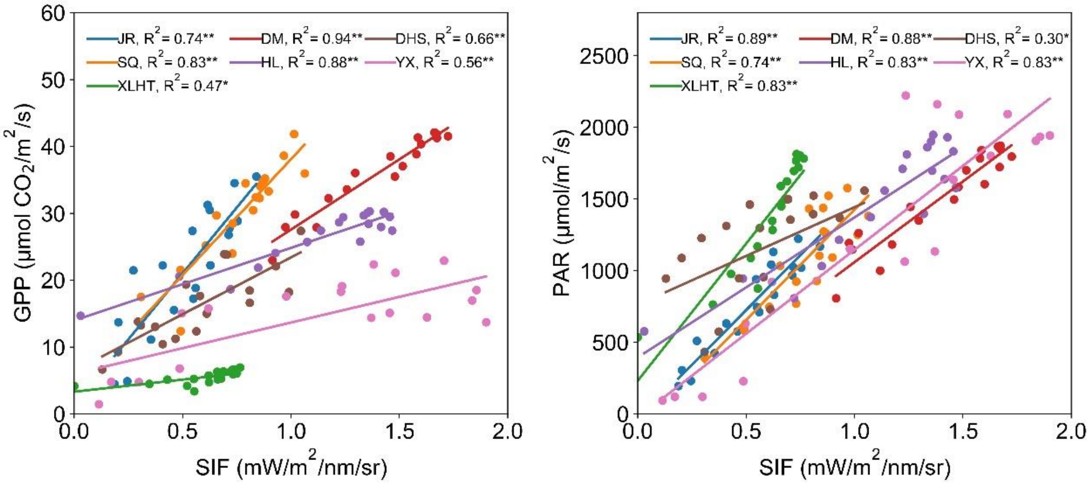

Figure 7. The diurnal relationship between SIF and GPP across multiple sites from one-day measurements under clear-sky conditions. The name of each site is referring in Table 1.

4.3 Validation of the fluorescence models with ground SIF observations

A number of fluorescence models have been developed and used in the SIF and carbon cycle community. Long term ground SIF measurements are valuable for validating these models. The Soil-Canopy Observation Photosynthesis and Energy fluxes (SCOPE) model is a widely-used model to simulate SIF at the site level (Van der Tol et al., 2009). To conduct the regional and global SIF simulations, the fluorescence models have been simplified and incorporated into several terrestrial biosphere models (Lee et al., 2015; Qiu et al., 2019). Recently, an efficient scheme accounting for the canopy scattering of SIF has been developed and implemented into the Boreal Ecosystem Productivity Simulator (BEPS-SIF) (Qiu et al., 2019). Generally, the satellite-based SIF measurements are used for the validations of above-mentioned models. However, satellites just measured SIF only at a snapshot of a day (e.g., GOME-2 at 9:30 and TROPOMI at 13:30) and the satellite-based SIF measurements have limitations for validating the diurnal simulations of these models. Therefore, long term *in situ* measurements are important for the developments of the fluorescence models. Hourly and daily SIF observations from three sites (JR-rice, SQ-maize and XLHT-grassland) are compared with SIF simulations by SCOPE and BEPS-SIF model. Figure 8 shows the scatter plots between observed SIF and simulated SIF from SCOPE and BEPS-SIF at both hourly and daily scale. For all the three sites, SIF simulations from two models are significantly correlated with ground observations, though the relationship between BEPS-SIF simulation and observation is slightly scattered than that between SCOPE simulation and observation. The SCOPE model accounts for complex radiative transfer process of SIF at the canopy level, while BEPS-SIF model used an effective way to calculate the canopy scattering of fluorescence (Qiu et al., 2019). This result demonstrates that these two models are effective to simulate SIF at both hourly and daily scales. The equally well performance of BEPS-SIF with SCOPE also proves its effectiveness for regional and global SIF simulations. Besides the model validations, the ground-based SIF measurements also improve the mechanistic understanding of photosynthetic activity, which is important for SIF representation within land surface models. For example, SIF measurements at a subalpine forest in Colorado are used to account for sustained NPQ in the SIF model, which largely improves the seasonal variations of SIF simulations for evergreen conifer forest (Raczka et al., 2018). This comparison between observations and simulations demonstrates the potential of continuous ground SIF observations for validating fluorescence models across multiple temporal scales.

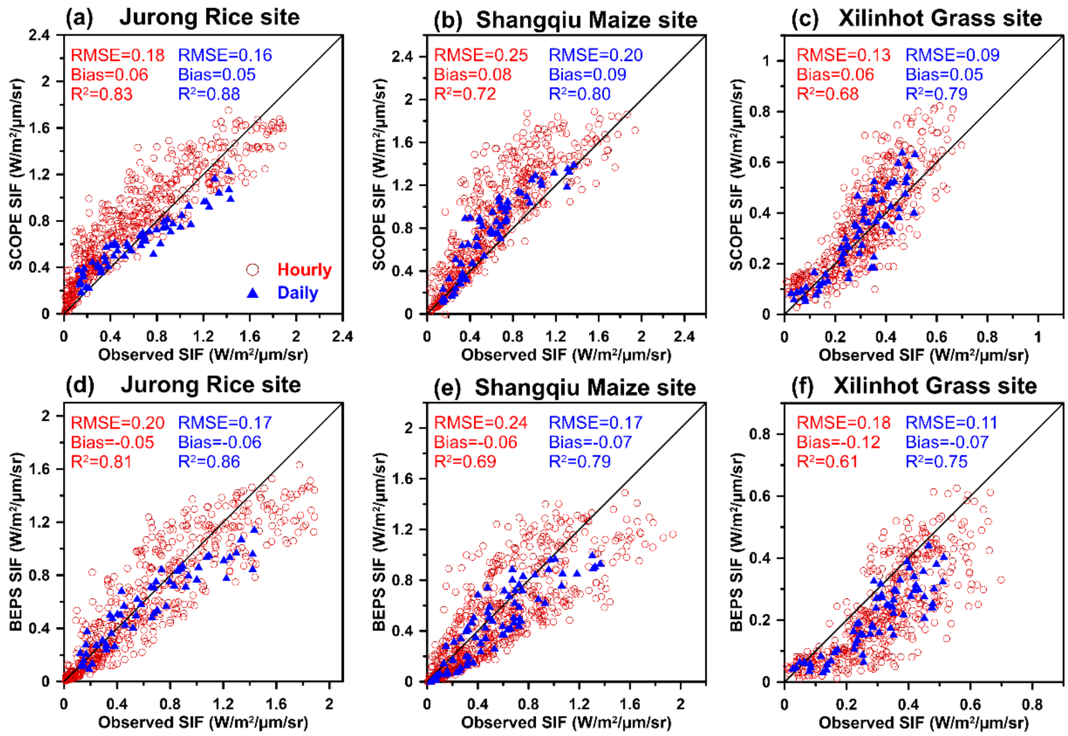

Figure 8. Validation of the fluorescence models using in situ SIF measurements for (a-c) SCOPE model and (d-f) BEPS-SIF model. The name of each site is referring in Table 1.

4.4 Validation of satellite SIF observations at the ground scale

A number of spaceborne sensors (e.g., GOME-2, OCO-2 and TROPOMI) have been used to retrieve SIF from space (Joiner et al., 2013; Köhler et al., 2015; Köhler et al., 2018; Sun et al., 2018; Du et al., 2018). The validation of satellite SIF retrieval with ground measurements of SIF is necessary for better understanding the canopy SIF signal. The fine spatial resolution of OCO-2 and TROPOMI SIF have facilitated the comparison with ground measurements. Here, five relatively homogeneous ground sites from ChinaSpec network, including four croplands (JR, HL, DM, and SQ) and one grassland (XLHT), are chosen to compare with the SIF retrievals from TROPOMI and OCO-2 satellites. These sites have overlap with the swath from both OCO-2 and TROPOMI. The land cover types around ground sites (shown in pentagram) with buffers of 10 km (black), 30 km (blue), and 50 km (red) radius are shown in Figure 9. Although the OCO-2 SIF products are provided in a high spatial resolution (1.3×2.25 km^2), its spatial coverage is not contiguous with only a handful of revisits within one year. Compared to OCO-2 SIF, TROPOMI SIF enables nearly daily global coverage due to its wide swath (~2600 km), in the cost of the coarse spatial resolution (7×3.5 km^2 at nadir). To compare with ground-based observations, both TROPOMI and OCO-2 SIF observations were averaged from all available data within a 50 km-buffer around the site (red circle in Figure 9). Taking OCO-2 SIF as an example, all available observations (black dot) from 2014 to 2018 are also shown in Figure 9.

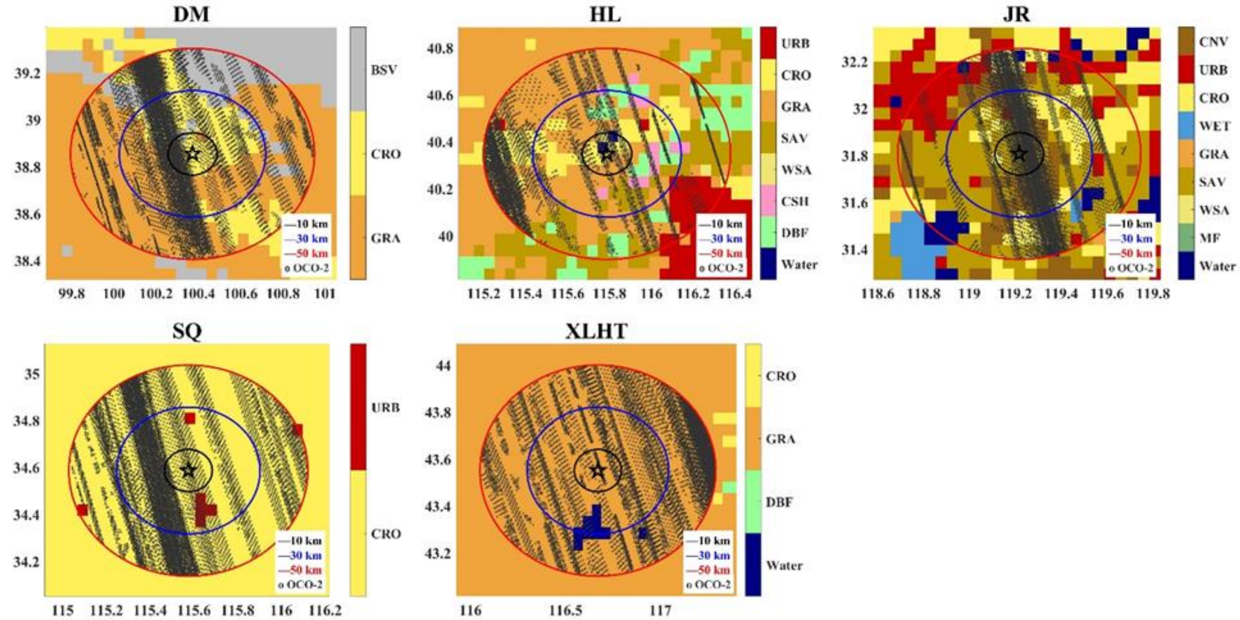

Figure 9. Surrounding land cover and available OCO-2 observations with buffers of 10 km, 30 km and 50 km radius of five ground-based SIF observation sites (DM, HL, JR, SQ and XLHT). The base map is the MODIS Land Cover product (MCD12C1 v6) with the IGBP land cover classification scheme. The black dots are OCO-2 overpasses at individual sites from 2014 to 2018.

The seasonal variations of SIF retrievals from ground observations and two satellite platforms are shown in Figure 10, displaying the seasonal SIF values of each day at the overpass local time of ~1:30 pm for OCO-2 and TROPOMI. As for OCO-2 SIF with a coarse temporal resolution (16 days), multi-year (2014-2018) mean data are used as the climatic mean SIF. In addition, TROPOMI SIF at 740 nm was multiplied by 0.67 to be compatible with ground SIF at 760 nm (Yang et al., 2015). The small difference between SIF at 757 nm (OCO-2) and 760 nm were ignored. Generally, these three SIF observations showed similar seasonal variations although ground measurements of SIF has higher day-to-day variations than spaceborne SIF. Overall, both OCO-2 and TROPOMI SIF show consistent seasonal amplitudes with ground measurements of SIF. Considering that there are still mismatch of the footprint between satellite and ground measurements, such seasonal consistence already indicates the usefulness of ground SIF measurements in ChinaSpec.

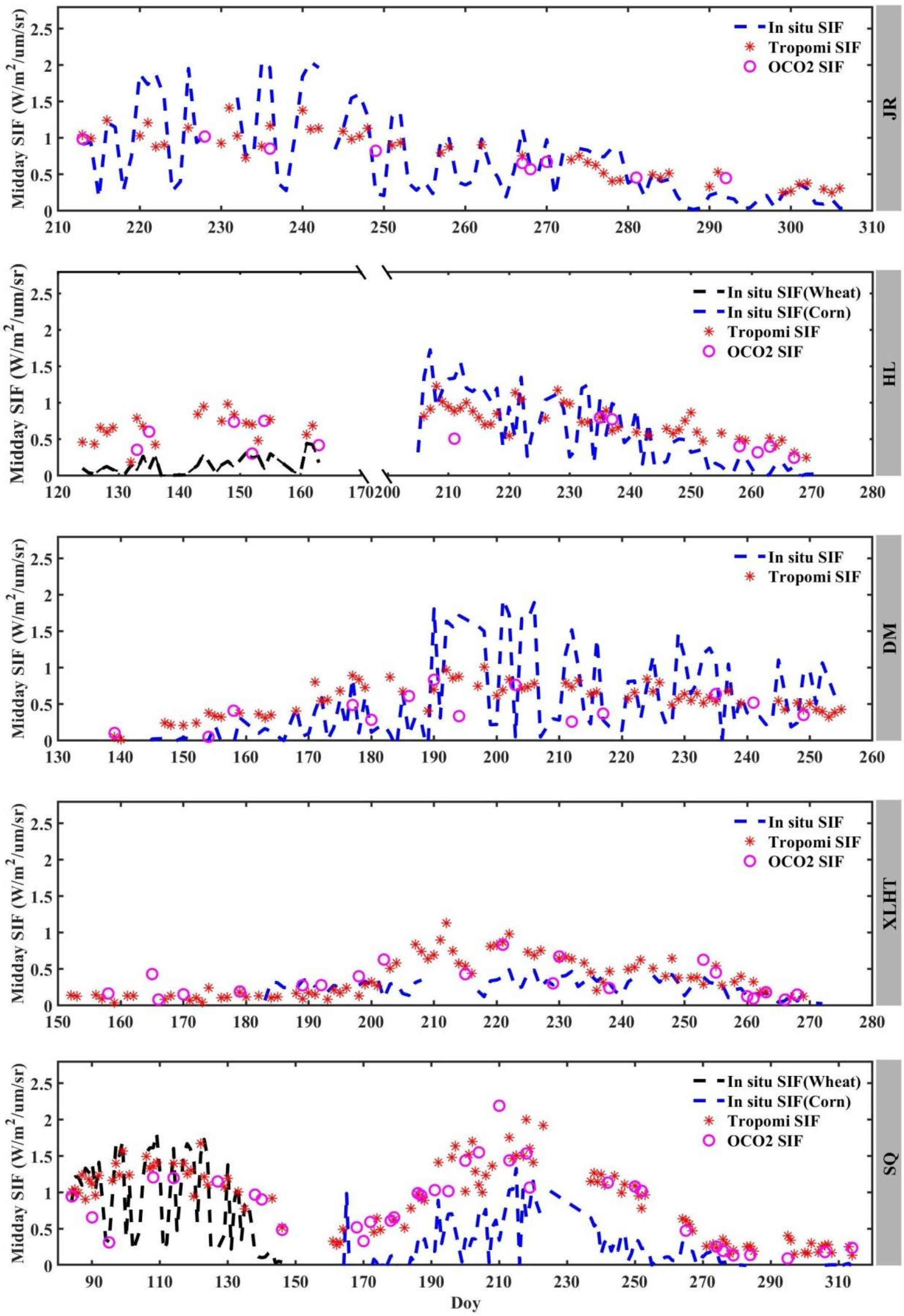

Figure 10. Comparison of seasonal variations of ground-based and spaceborne (TROPOMI and OCO-2) SIF observations at five SIF sites. The name of each site is referring in Table 1.

Further demonstration of the correlation between satellite SIF observations (TROPOMI) and ground SIF is shown in Figure 11. Significant relationships ($p<0.001$) between TROPOMI SIF retrievals and ground measurements of SIF were observed for all sites except for HL during the growing season of maize. The correlations (R^2) vary across different sites, ranging from the minimal of 0.34 at XLHT to the maximal of 0.75 at JR. The highest R^2 for in situ SIF and TROPOMI SIF in JR indicate satellite retrievals at this place are accurate. Similar results were also observed at the SQ site during both wheat and maize seasons. However, at HL and DM, the relationships between in situ SIF and TROPOMI SIF were clearly weaker than that at JR and SQ. The possible reason is the mismatch of footprints between TROPOMI SIF and ground measurements of SIF. The lowest R^2 (0.34) was observed at XLHT probably due to the grazing management around the XLHT site within a 50 km radius although the surrounding land cover (grassland) is homogeneous. In addition, the SIF retrievals with low values in grassland are easy to be affect by the retrieval noise, causing the relatively weak correlation between ground and satellite SIF for XLHT. These results suggest the potential and also the challenges for the validation of different satellite SIF observations with ground SIF measurements.

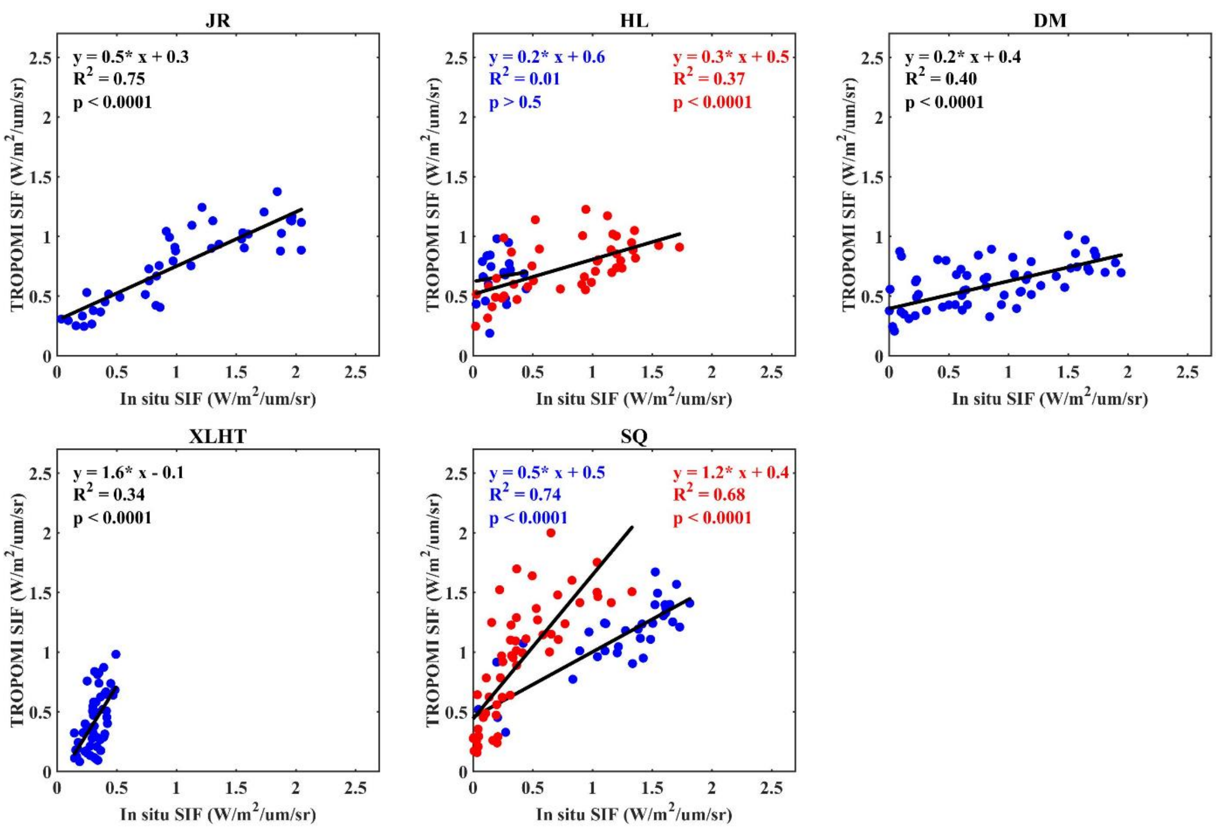

Figure 11. Comparison of in situ and satellite SIF measurements at multiple sites. TROPOMI SIF calculated for 740 nm was converted to 760 nm by multiplying 0.67. For the HL and SQ sites, red and blue dots represent wheat and maize, respectively.

5 Outlook and challenges

5.1 Standardization of instrument configurations and data processing

A number of challenges still exist for effectively integrating optical (including SIF) and EC flux measurements. The lack of standardization is probably the most concerns among the challenges (Porcar-Castell et al., 2015). Currently, different sensors are applying to *in situ* continuous spectral measurements at the EC sites in the network of ChinaSpec. Plenty of spectral data of different resolutions have been collected in different formats with a variety of properties. To facilitate the utilization of remote sensing for monitoring carbon cycle across different systems, optical measurements (especially SIF) would better to be conducted following a standard protocol from the very beginning of instrument setup to data processing and analysis.

Attribute to development of optical measurement technology, the spectral resolution of spectrometer for reflectance measurements (for calculating VI) reach up to 1~3 nm and that for SIF observations achieve less than 0.3 nm with high signal-to-noise ratio. These kinds of spectrometers are recommended to be used to improve the data quality from different sites and to simplify the data normalization of different spectral resolutions and ranges. For field setup, solar and canopy radiation should be simultaneously acquired using the same spectrometer to avoid spectral shifting from two sensors. Cosine corrector of the solar irradiance measurements is suggested to be conducted for long term observations. Canopy radiation has two options to be measured, i.e. hemispherical cosine corrector or conical bare fiber, depending on the canopy structure. The hemispherical configurations could enlarge the field of view to represent the average condition of the canopy and also to reduce the signal from non-vegetation factors. Conical measurement of radiance is suitable for homogeneous canopy, and hemispherical measurement of irradiance is appropriate to heterogeneous canopy (Zhang et al., 2019).

Data collection and storage may be conducted in different ways, but the information include raw DN, IT and DC should be recorded for post-retracing and investigating the status of the observation system. The same data processing and analysis techniques are also needed to better standardize the SIF measurements across sites. As mentioned in Section 2.1, the raw data should be corrected (dark current) and calibrated (radiometric calibration), as well as quality controlled following a standard procedure for reflectance calculation and SIF retrievals. We suggest that the output data for sharing at least consists of solar and canopy radiation, reflectance and SIF retrievals using 3FLD and SFM. A suitable metadata is necessary to describe the information about the site, observation system and data structure, etc.

5.2 Linking remote sensing with EC flux measurements in China

An opportunity to investigate the ability of SIF and hyperspectral reflectance to monitor biosphere-atmosphere carbon exchange with round-the-clock synthetic spectra and carbon flux observations under all weather conditions benefits from the development of high-resolution spectroscopy technique (Porcar-Castell et al., 2015). The development of the ChinaSpec network collaborating with ChinaFLUX network (Yu et al., 2006; Yu et al., 2010) will help bridge the integration of EC flux measurements and remote sensing. The high frequency *in situ* SIF and hyperspectral reflectance can complement the long-tern EC carbon and water flux measurements, and help to bridge *in situ* observation and satellite products for carbon flux prediction at regional scales over a variety of ecosystems in China, which indicates the urgent expansion of the ChinaSpec network. Besides, the development of ChinaSpec Networks of ground-based sensors will also benefit the utility of upscaling the ground measurements to regional and global scales based on existing upscaling approaches and the current satellite remote sensing data. Ground-based SIF retrievals also provide a non-invasive way to track the seasonality and spatial patterns of vegetation phenology, such as providing observations of individual vegetation spectral, as a way of being proxies to predict vegetation optical properties (e.g., plant physiology and biochemistry) and further monitoring vegetation photosynthetic changes. All these measurements and proxies have shown great promise for linking ground-based optical observations and the satellite phenology data.

A number of airborne and spaceborne sensors with high-spectral resolution enable the retrievals of SIF at regional and global scales, including GOSAT, GOME-2, OCO-2, OCO-3, TROPOMI, FLEX, and GeoCARB (Frankenberg et al., 2011; Joiner et al., 2013; Köhler et al., 2015; Köhler et al., 2018; Sun et al., 2018; Guanter et al., 2012; Drusch et al., 2017). Therefore, it is urgent to develop *in situ* measurements of SIF in parallel to validate the accuracy of SIF retrievals from satellite or airborne platforms. Most of the current satellite SIF is measured at a certain time of a day (e.g., GOME-2 local overpass time is around 9:30 a.m.), except for GeoCARB and OCO-3 that can continuously measure SIF on a daily basis. Therefore, the validation of satellite-based SIF can provide robust information on regional to global-scale plant photosynthetic function and provide powerful force to the ecosystem photosynthesis monitoring from satellite remote sensing. Concurrently, comparisons with ground-based SIF also constitute an important component in the calibration of various SIF-based photosynthesis models (e.g., SCOPE). In addition, the information of red SIF retrieval has been investigated for ground SIF measurement but is not available for most current satellite SIF observation. Since red SIF contains more information of the photosystem II, therefore, the knowledge obtained from ground measurements will facilitate the retrieval of red SIF at the satellite platform to achieve a combination of red SIF and far red SIF, which is important to the mechanism of SIF emitted by vegetation.

Both satellite and ground-based SIF observations have shown the potential to quantify plant photosynthetic activities and stresses at the ecosystem scale. Although satellite SIF has shown to be a good proxy for GPP, the existence of scale mismatch between satellite SIF and flux tower GPP hinders the fully use of SIF to constrain GPP at the global scale. Therefore, a promotion of establishing more ground-based SIF observation systems is important to fully characterize the relationship between SIF and GPP by obtaining synchronous SIF continuous observations and CO2 flux measurements across different terrestrial ecosystems and to understand photosynthetic activities of terrestrial ecosystems. Furthermore, long term ground-based SIF measurements have the potentials to study the diurnal and seasonal changes in GPP across different biomes, canopy structures and environmental conditions, which is not available for the current satellite due to the discrete temporal samplings and instrumental difference among different satellite. However, the footprint mismatch between optical and flux observations urges the representative of spectral observation or post-process to make the optical signal represent the average condition of the whole canopy just like the EC measurements do.

6 Summary

Taking advantage of new advances of spectroscopy technique, automatic spectral observation system can be performed to continuously measure ground canopy reflectance and especially SIF, which are efficient approaches to monitor the carbon budget of terrestrial ecosystems. Attribute to collaboration of several institutes conducting *in situ* hyperspectral and SIF measurements at high temporal resolution using automatic systems in China, the network of ChinaSpec was established. The network currently is consisting of 15 sites including 5 cropland sites, 4 grassland sites, 4 forest sites and 2 wetland sites. Here, we specifically described the details of instrument configurations, data collection and processing procedures, data sharing and utilization protocols. Based on data acquired from some sites in last two years, we show examples how the SIF observations can be used to track vegetation photosynthesis from diurnal to seasonal scale, to validate the fluorescence models and satellite SIF retrievals (e.g., from OCO-2 and TROPOMI). ChinaSpec is dedicated to facilitate integration of spectral and flux measurements for better monitoring and predicting carbon exchange between the atmosphere and biosphere, and benefits both remote sensing and ecology research communities. Still, there are many challenges in expanding the network and in reaching a standard protocol from data acquisition, processing to utilization. This necessarily requires broader collaborations from interested researchers or groups to advance this research area.

Acknowledgments

This research was supported by the National Key R&D Program of China (2019YFA0606601, 2017YFC0503800), the General Program of Natural Science Foundation of China (41671421), and the International Cooperation and Exchange Programs between Natural Science Foundation of China and DFG of Germany (41761134082). We would thank Dr. Zhongyang Li, Dr. Hezhou Wang, and Mr. Pengju Wu and other researchers from National Agro-Ecological Observation and Research Station of Shangqiu, Henan, China for the field measurements. These students involved in the data collection were also acknowledged. We would also like to acknowledge the NASA Earth Science Data Systems program for the MODIS and OCO-2 products (https://search.earthdata.nasa.gov/). The TROPOMI SIF data providers, Prof. Philipp Koehler and Prof. Christian Frankenberg, were also acknowledged (ftp://fluo.gps.caltech.edu/data/tropomi/). We also greatly appreciate the ChinaFLUX for providing EC flux data (http://www.chinaflux.org/index.aspx).

References

Alonso, L., Gómez-Chova, L., Vila-Francés, J., Amorós-López, J., Guanter, L., Calpe, J., et al. (2008). Improved Fraunhofer Line Discrimination method for vegetation fluorescence quantification. IEEE Geoscience and Remote Sensing Letters, 5(4), 620–624. https://doi.org/10.1109/LGRS.2008.2001180.

Baldocchi, D. (2008). Breathing of the terrestrial biosphere: lessons learned from a global network of carbon dioxide flux measurement systems, Aust. J. Bot., 56, 1–26, https://doi.org/10.1071/bt07151.

Baldocchi, D. (2019). How eddy covariance flux measurements have contributed to our understanding of Global Change Biology. Global Change biology, 00, 1-19, https://doi.org/10.1111/gcb.14807.

Cogliati, S., Rossini, M., Julitta, T., Meroni, M., Schickling, A., Burkart, A., et al. (2015). Continuous and long-term measurements of reflectance and sun-induced chlorophyll fluorescence by using novel automated field spectroscopy systems. Remote Sensing of Environment, 164, 270-281. https://doi.org/10.1016/j.rse.2015.03.027.

Damm, A., Guanter, L., Paul-Limoges, E., van der Tol, C., Hueni, A., Buchmann, N., et al. (2015). Far-red sun-induced chlorophyll fluorescence shows ecosystem-specific relationships to gross primary production: An assessment based on observational and modeling approaches. Remote Sensing of Environment, 166, 91-105. https://doi.org/10.1016/j.rse.2015.06.004.

Drusch, M., Moreno, J., Del Bello, U., Franco, R., Goulas, Y., Huth, A., et al. (2017). The fluorescence explorer mission concept—ESA's Earth explorer 8. IEEE Transactions on Geoscience and Remote Sensing, 55, 1273-1284. https://doi.org/10.1109/TGRS.2016.2621820.

Du, S., Liu, L., Liu, X., Guo, J., Hu, J., Wang, S., & Zhang, Y.(2019). SIFSpec: Measuring Solar-Induced Chlorophyll Fluorescence Observations for Remote Sensing of Photosynthesis. Sensors, 19, 3009. https://doi.org/10.3390/s19133009.

Du, S., Liu, L., Liu, X., Zhang, X., Zhang, X., Bi, Y., & Zhang, L. (2018) Retrieval of global terrestrial solar-induced chlorophyll fluorescence from TanSat satellite. Science Bulletin, 63, (22), 1502-1512. https://doi.org/10.1016/j.scib.2018.10.003.

Frankenberg, C., Fisher, J. B., Worden, J., Badgley, G., Saatchi, S. S., Lee, J. E., et al. (2011). New global observations of the terrestrial carbon cycle from GOSAT: Patterns of plant fluorescence with gross primary productivity. Geophysical Research Letters, 38, 351-365. https://doi.org/10.1029/2011GL048738.

Gamon, J. A., Coburn, C., Flanagan, L. B., Huemmrich, K. F., Kiddle,C., Sanchez-Azofeifa, G. A., et al. (2010). SpecNet revisited: bridging flux and remote sensing communities. Canadian Journal of Remote Sensing, 36, S376–S390. https://doi.org/10.5589/m10-067.

Gamon, J. A., Rahman, A. F., Dungan, J. L., Schildhauer, M., & Huemmrich, K. F. (2006) Spectral Network (SpecNet) – what is it and why do we need it? Remote Sensing of Environment, 103, 227–235. https://doi.org/10.1016/j.rse.2006.04.003.

Gómez-Chova, L., Alonso, L., Amorós-López, J., Vila-Francés, J., del Valle-Tascón, S., Calpe, J., et al. (2006). Solar-induced fluorescence measurements using a field spectroradiometer. Earth observation for vegetation monitoring and water management. AIP Conference Proceedings, 852, 274–281. https://doi.org/10.1063/1.2349354.

Grossmann, K., Frankenberg, C., Magney, T. S., Hurlock, S. C., Seibt, U., & Stutz, J. (2018). PhotoSpec: A new instrument to measure spatially distributed red and far-red Solar-Induced Chlorophyll Fluorescence. Remote Sensing of Environment, 216, 311–327. https://doi.org/10.1016/j.rse.2018.07.002.

Gu, L., Wood, J. D., Chang, C. Y. Y., Sun, Y., & Riggs, J. S. (2019). Advancing Terrestrial Ecosystem Science With a Novel Automated Measurement System for Sun-Induced Chlorophyll Fluorescence for Integration With Eddy Covariance Flux Networks. Journal of Geophysical Research: Biogeosciences, 124(1), 127–146. https://doi.org/10.1029/2018JG004742.

Guanter, L., Frankenberg, C., Dudhia, A., Lewis, P.E., Gómez-Dans, J., Kuze, A., et al. (2012). Retrieval and global assessment of terrestrial chlorophyll fluorescence from GOSAT space measurements. Remote Sensing of Environment, 121, 236-251. https://doi.org/10.1016/j.rse.2012.02.006.

Guanter, L., Zhang, Y., Jung, M., Joiner, J., Voigt, M., Berry, J.A., et al. (2014). Global and time-resolved monitoring of crop photosynthesis with chlorophyll fluorescence. Proceedings of the National Academy of Sciences of the United States of America, 111, E1327-E1333. https://doi.org/10.1073/pnas.1320008111.

Hilker, T., Coops, N. C., Wulder, M. A., Black T. A., & Guy R. D. (2008). The use of remote sensing in light use efficiency based models of gross primary production: a review of current status and future requirements. Science of the Total Environment, 404, 411–423. https://doi.org/10.1016/j.scitotenv.2007.11.007.

Huete, A. R., Didan, K., Miura, T., Rodriguez, E. P., Gao, X., & Ferreira, L. G. (2002), Overview of the radiometric and biophysical performance of the MODIS vegetation indices. Remote Sensing of Environment, 83, 195–213. https://doi.org/10.1016/S0034-4257(02)00096-2.

Joiner, J., Guanter, L., Lindstrot, R., Voigt, M., Vasilkov, A. P., Middleton, E. M., et al. (2013). Global monitoring of terrestrial chlorophyll fluorescence from moderate-spectral-resolution nearinfrared satellite measurements: methodology, simulations, and application to GOME-2. Atmospheric Measurement Techniques, 6, 2803-2823. https://doi.org/10.5194/amt-6-2803-2013.

Köhler, P., Frankenberg, C., Magney, T. S., Guanter, L., Joiner, J., & Landgraf, J. (2018). Global retrievals of Solar-Induced Chlorophyll Fluorescence with TROPOMI: First results and intersensor comparison to OCO-2. Geophysical Research Letters, 45, 10456-10463. https://doi.org/10.1029/2018GL079031.

Köhler, P., Guanter L., Joiner J. (2015), A linear method for the retrieval of sun-induced chlorophyll fluorescence from gome-2 and sciamachy data, Atmospheric Measurement Techniques, 8(6), 2589-2608. https://doi.org/10.5194/amt-8-2589-2015.

Lee, J. E., Berry, J. A., van der Tol, C., Yang, X., Guanter, L., Damm, A., et al. (2015). Simulations of chlorophyll fluorescence incorporated into the Community Land Model version 4. Global Change Biology, 21, 3469–3477. https://doi.org/10.1111/gcb.12948.

Li, Z., Zhang, Q., Li, J., Yang, X., Wu, Y., Zhang, Z., et al. (2020). Solar-induced chlorophyll fluorescence and its link to canopy photosynthesis in maize from continuous ground measurements. Remote Sensing of Environment, 2020, 236, 111420. https://doi.org/10.1016/j.rse.2019.111420.

Magney, T. S., Frankenberg, C., Köhler, P., North, G., Davis, T. S., Dold, C., et al. (2019). Disentangling Changes in the Spectral Shape of Chlorophyll Fluorescence: Implications for Remote Sensing of Photosynthesis. Journal of Geophysical Research: Biogeosciences. https://doi.org/10.1029/2019JG005029.

Maier, S. W., Günther, K. P., & Stellmes, M. (2003). Sun-induced fluorescence: A new tool for precision farming. In T. VanToai, D. Major, M. McDonald, J. Schepers, & L. Tarpley (Eds.), Digital imaging and spectral techniques: Applications to precision agriculture and crop physiology (pp. 209–222). Madison: American Society of Agronomy. https://doi.org/10.2134/asaspecpub66.c16.

Meroni, M., & Colombo, R. (2006). Leaf level detection of solar induced chlorophyll fluorescence by means of a subnanometer resolution spectroradiometer. Remote Sensing of Environment, 103, 438–448. https://doi.org/10.1016/j.rse.2006.03.016.

Meroni, M., Rossini, M., Guanter, L., Alonso, L., Rascher, U., Colombo, R., et al. (2009). Remote sensing of solar-induced chlorophyll fluorescence: review of methods and applications. Remote Sensing of Environment, 113(10), 2037-2051. https://doi.org/10.1016/j.rse.2009.05.003.

Moya, I., Ounis, A., Moise, N., & Goulas, Y. (2006). First airborne multiwavelenght passive chlorophyll fluorescence measurements over La Mancha (Spain) fields. In J. A. Sobrino (Ed.), Second recent advances in quantitative remote sensing (pp. 820–825). Spain: Publicacions de la Universitat de València. https://doi.org/10.13140/2.1.1031.9364.

Porcar-Castell, A., Mac Arthur, A., Rossini, M., Eklundh, L., Pacheco-Labrador, J., Anderson, K., et al. (2015). EUROSPEC: at the interface between remote-sensing and ecosystem CO_2 flux measurements in Europe. Biogeosciences, 12(20):6103-6124. https://doi.org/10.5194/bg-12-6103-2015.

Qiu, B., Chen, J. M., Ju, W., Zhang, Q., Zhang, Y. (2019). Simulating emission and scattering of solar-induced chlorophyll fluorescence at far-red band in global vegetation with different canopy structures. Remote Sensing of Environment, 233, 111373. https://doi.org/10.1016/j.rse.2019.111373.

Quan, Q., Tian, D., Luo, Y., Zhang, F., Crowther. T. W., Zhu, K., et al. (2019). Water scaling of ecosystem carbon cycle feedback to climate warming. Science Advances, 5(8): evva1131. https://doi.org/10.1126/sciadv.aav1131.

Raczka, B., Porcar-Castell, A., Magney, T., Lee, J. E., Köhler, P., Frankenberg, C., et al. (2018). Sustained Non-Photochemical Quenching Shapes the Seasonal Pattern of Solar-Induced Fluorescence at a High-Elevation Evergreen Forest. Journal of Geophysical Research: Biogeosciences, 124(7), 2005-2020. https://doi.org/10.1029/2018JG004883.

Shan, N., Ju, W. M., Migliavacca, M., Martini, D., Guanter, L., Chen, J. M., et al. (2019), Modeling canopy conductance and transpiration from solar-induced chlorophyll fluorescence, Agri. Forest Meterol., 268, 189-201. https://doi.org/10.1016/j.agrformet.2019.01.031.

Sun, Y., Frankenberg, C., Jung, M., Joiner, J., Guanter, L., Köhler, P., & Magney, T. (2018). Overview of Solar-Induced chlorophyll Fluorescence (SIF) from the Orbiting Carbon Observatory-2: Retrieval, cross-mission comparison, and global monitoring for GPP. Remote Sensing of Environment, 209, 808-823. https://doi.org/10.1016/j.rse.2018.02.016.

Theisen, A. F. (2002). Detecting chlorophyll fluorescence from orbit: The Fraunhofer Line Depth model. In R. S. Muttiah (Ed.), From Laboratory Spectroscopy to Remotely Sensed Spectra of Terrestrial Ecosystems (pp. 203–232). Dordrecht: Kluwer Academic Publishers1-4020-0753-1. https://doi.org/10.1007/978-94-017-1620-8_10.

Tong, X., Mu, Y., Zhang, J., Meng, P., &Li, J., (2019). Water stress controls on carbon flux and water use efficiency in a warm-temperate mixed plantation. Journal of Hydrology, 571, 669-678. https://doi.org/10.1016/j.jhydrol.2019.02.014.

Van der Tol, C., Verhoef, W., Timmermans, J., Verhoef, A., & Su, Z. (2009). An integrated model of soil-canopy spectral radiances, photosynthesis, fluorescence, temperature and energy balance. Biogeosciences, 6, 3109–3129. https://doi.org/10.5194/bg-6-3109-2009.

Wang, H., Han, D., Mu, Y., Jiang, L., Yao, X., Bai, Y., et al. (2019). Landscape-level vegetation classification and fractional woody and herbaceous vegetation cover estimation over the dryland ecosystems by unmanned aerial vehicle platform. Agricultural and Forest Meteorology, 278, 107665. https://doi.org/10.1016/j.agrformet.2019.107665.

Wang, C., Yu, G., Zhou, G., Yan, J., Zhang, L., Wang, X., et al. (2006). CO2 flux evaluation over the evergreen coniferous and broad-leaved mixed forest in Dinghushan, china. Science in China, 49(2 Supplement), 127-138. https://doi.org/10.1007/s11430-006-8127-3.

Yang, P., Luo, J., Yuan, D., & He, Q. (2009). Response of spring water hydrochemical behaviors to rainfall in karst subterranean river system. Journal of Hydraulic Engineering, 40(1): 67-74. https://doi.org/10.3321/j.issn:0559-9350.2009.01.010.

Yang, K., Ryu, Y., Dechant, B., Berry, J.A., Hwang, Y., Jiang, C., et al. (2018a). Sun-induced chlorophyll fluorescence is more strongly related to absorbed light than to photosynthesis at half-hourly resolution in a rice paddy. Remote Sensing of Environment, 216, 658-673. https://doi.org/10.1016/j.rse.2018.07.008.

Yang, X., Shi, H., Stovall, A., Guan, K., Miao, G., Zhang, Y., et al. (2018b). FluoSpec 2-An automated field spectroscopy system to monitor canopy solar-induced fluorescence. Sensors, 18, 2063. https://doi.org/10.3390/s18072063.

Yang, X., Tang, J., Mustard, J. F., Lee, J.-E., Rossini, M., Joiner, J., et al. (2015). Solar-induced chlorophyll fluorescence that correlates with canopy photosynthesis on diurnal and seasonal scales in a temperate deciduous forest. Geophysical Research Letters, 42, 2977-2987. https://doi.org/10.1002/2015GL063201.

Yu, G.R., Wen, X.F., Sun, X. M., Tanner, B.D., Li, X., & Chen, J.Y. (2006). Overview of ChinaFLUX and evaluation of its eddy covariance measurement. Agricultural and Forest Meteorology, 137, 125-137. https://doi.org/10.1016/j.agrformet.2006.02.011.

Yu, G.R., Zhang, L.M., Su, X. M., (2010). Progresses and prospects of Chinese terrestrial ecosystem flux observation and research network (ChinaFLUX). Progress in Geography, 33(7), 903-917. https://doi.org/10.11820/dlkxjz.2014.07.005.

Zhang, Q., Zhang, X., Li, Z., Wu, Y., & Zhang, Y. (2019). Comparison of Bi-Hemispherical and Hemispherical-Conical Configurations for In Situ Measurements of Solar-Induced Chlorophyll Fluorescence. Remote Sensing, 11, 2642. https://doi.org/10.3390/rs11222642.

Zhang, B., Li, S., Chen, S., Ren, T., Yang, Z., Zhao, H., et al. (2016). Arbuscular mycorrhizal fungi regulate soil respiration and its response to precipitation change in a semiarid steppe. Scientific Report, 6, 19990. https://doi.org/10.1038/srep19990.